

STUDY ON PROTECTION MEASURES FOR SEISMIC ISOLATION RUBBER BEARINGS

Xi-Yuan Zhou*, Miao Han** and Lin Yang***

*Beijing Laboratory of Earthquake Engineering and Structural Retrofit
Beijing University of Technology, Pingleyuan No. 100, Beijing 100022, P.R.C.

**Beijing Institute of Civil Engineering and Architecture, Beijing 100044, P.R.C.

***Hebei Institute of Technology, Tangshan, Hebei 063000, P.R.C.

ABSTRACT

In a base-isolated building, the rubber bearings, being as protectors of the superstructure, sometimes should also be protected from failure because the failure of rubber bearings may result in serious damage to superstructure. In this paper, three failure-prevention approaches of rubber bearings are proposed. The simplest way is to limit maximum stroke of rubber bearings with stoppers and buffers. This is called soft pounding protection. Another way is to arrange additional stiffness components at abutments in certain distance from the protected rubber bearings, which is called stiffness variable protection. The third way is to install backup supporters with friction sliding plate on their top beside rubber bearings. This is called soft landing protection. The principle, working mechanism and analytical models for these safeguard devices are studied. The effectiveness of these approaches for protecting rubber bearings is discussed by examples.

KEYWORDS: Seismic Isolation, Soft Pounding, Stiffness Variable Protection, Soft Landing, Rubber Bearing

INTRODUCTION

The fundamental principle of base isolation is to set a flexible layer between superstructure and footing base. Flexibility of the isolation layer causes the fundamental period of a given structure to be extended to a value far away from the dominant period contents of earthquake ground motion ranging from 0.1 to 1.0 sec so that the earthquake-induced loading will be greatly reduced. Theoretically, the fundamental period of base-isolated structure should be as long as possible to avoid this period range through lowering the stiffness of isolation system, but it might result in a large horizontal displacement. Also, the rubber bearing must have sufficiently large deformation capacity to undertake this large horizontal displacement. Using large diameter rubber bearings can give required large lateral deformation capacity, but the horizontal stiffness and cost of the isolation system increase consequently. The rubber bearings of relatively small diameter can both lengthen the period of the structure and reduce the cost of isolation system, but its lateral stability during a strong earthquake sometimes would be a problem. In consideration of these factors, as mentioned above, the fundamental period of the base-isolated buildings usually is kept as 2.0 sec. But, sometimes, the fundamental period of base-isolated structures has been extended to 3.0-4.0 sec to avoid the possible long period resonance. However, if relatively small diameter rubber bearings are adopted that probably have no sufficient lateral deformation capacity, during the extreme earthquake, adopting protect measures becomes necessary. In order to prevent failure of rubber under long period ground motions, Kelly et al. (1980) proposed a skid system, which provides hysteretic damping to protect rubber bearing and has been verified by shaking table testing. Moreover, the isolators in buildings are protected due to finite moat width (the isolation plane cannot displace more than the moat width), especially when the seismic input is much larger than the expected ground motions. The impact between building and moat is surely able to protect superstructures but simultaneously induces harsh accelerations or high frequency shocks in it. Hence, inserting mechanical buffers and dampers onto the gap between building and moat perhaps is a supplemental measure to abate such kind of shocks. In this paper, three measures for protecting rubber bearings are proposed: 1. soft pounding protection, 2. variable stiffness system, 3. soft landing protection. Options 1 and 2 in this paper will be excellent choices in softening the impact. The principle, working mechanism and analytical models for these safeguard devices are studied. The seismic response analyses of the base-isolated systems with rubber bearing

failure prevention measures are also carried out. The purpose of the study in this paper is to develop a more economical base isolation system by using relatively smaller rubber bearings, especially for fitting the need of small size buildings. Hence, isolators should be designed only for frequently or occasionally occurring moderate earthquakes, while those are allowed to be unstable at the maximum possible earthquake with reliance on the proposed protection devices to eliminate catastrophic failure. The analytical methods in this paper combined with future shake table tests may pave a way for such new design approach.

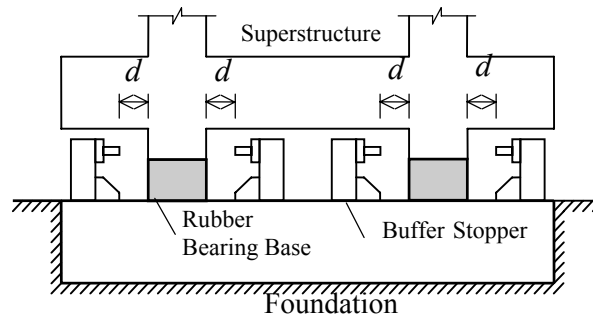


Fig. 1 Schematic diagram of buffer stopper

THE SOFT POUNDING PROTECTION

1. Fundamental Principle

The schematic diagram of a buffer stopper is shown in Figure 1, where d is the preset space between isolated structure and footing base. If the horizontal displacement of the isolation layer increases and reaches the prescribed value of d , the stopper will bump on the isolator, thus further increase of displacement of rubber bearings would be restricted. In contrast, without buffer between the isolator and the stopper, the so-called hard pounding will happen. In Kelly et al. (1980), the authors studied the isolation systems for a judicial building in California, the first base-isolated building with laminated rubber bearings in America, and concluded that the high frequency vibration caused by hard pounding is harmful to superstructure. Many theoretical and experimental studies on base isolation devices and isolator fail protection systems have been carried out in recent twenty years or so (Bruce and Carlos, 1992; Buckle and Kelly, 1986; Griffith et al., 1987; Han, 1997; Kelly et al., 1980; Kelly, 1998; Koh and Kelly, 1986; Nagarajaiah and Ferrell, 1999; Ohhira et al., 1990; Sun and Goto, 1996; Zhou et al., 1997; Zhou et al., 2000). In this paper, we introduce a system with a buffer and a stopper in parallel, called buffer stopper. When soft pounding happens, stoppers will undertake deformation and impose desirable reaction force onto the isolators, which, together with the restoring forces of the rubber bearings, will restrict the lateral deflection of rubber bearings within the allowable value.

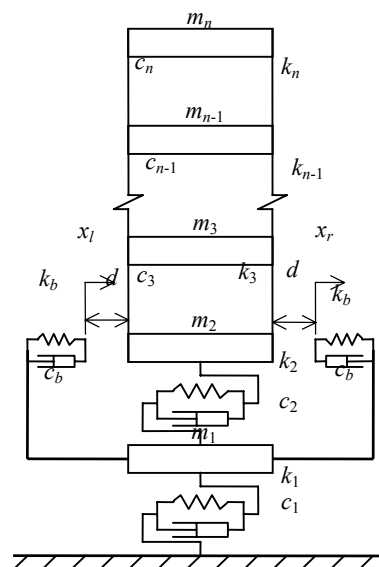


Fig. 2 Mechanical model (I)

2. Mechanical Model and Equations of Motion

In the course of soft pounding, the interaction force among stoppers and isolators is imparted to basement and then transmitted into the foundation through spring and damping devices. The model described here includes the effect of soil-structure interaction (see Figure 2), but only one-dimensional horizontal motion is concerned. The rocking and torsional effects of the soil-structure interaction system are neglected in this study.

The concerned building is regarded as a shear type structure. In Figure 2, m_i, k_i, c_i ($i = 3, \dots, n$) are the mass, stiffness coefficient and damping coefficient, respectively, for each storey of the superstructure (the corresponding fixed base structure), m_2, k_2, c_2 are the mass, stiffness coefficient and damping coefficient of the isolating layer, respectively, and m_1, k_1, c_1 are the mass of the basement, equivalent stiffness coefficient and damping coefficient of the soil, respectively, which are determined according to the five lumped parameters 2-DOF discrete model (Wolf and Somaini, 1986; Jean et al., 1990; Luan and Lin, 1996). The mass of the stopper is negligible, k_b, c_b are stiffness coefficient and damping coefficient respectively of isolation layer, d is the designed presetting free space of the stopper, and x_r and x_l are deformations of the right and left stopper respectively. However, pounding may repeatedly happen during an earthquake, so the stopper may have been deformed before one more bumping occurs. Nevertheless, both the values of x_r and x_l are zero when the first pounding takes place.

2.1 Equation of Motion without Pounding

If the isolators do not bump against the stoppers that means the stopper has no effects on the motion of the structure, then the model in Figure 2 turns into a normal shear structure. Thus, the equation of motion becomes

$$[M]\{\ddot{x}\} + [C]\{\dot{x}\} + [K]\{x\} = -[M]\{1\}\ddot{x}_g \tag{1}$$

where $[M]$ is a diagonal mass matrix of order $n \times n$, $[C], [K]$ are damping and stiffness matrices respectively of order $n \times n$. $\{x\}, \{\dot{x}\}, \{\ddot{x}\}$ are n -dimensional vectors of nodal relative displacement, velocity, acceleration, against ground, respectively, $\{1\}$ is the identity vector, and \ddot{x}_g is ground acceleration. We further suppose matrix $[C]$ complying with the property of proportional damping.

2.2 Equation of Motion for Right Pounding

When the interstorey displacement of the isolation layer is larger than the sum of the preset open space and the deformation of the right stoppers x_r , namely, $x_2 - x_1 > x_r + d$, the isolators will bump against the right stoppers. The equation of motion in this case is given by (Han, 1997)

$$[M]\{\ddot{x}\} + [\bar{C}]\{\dot{x}\} + [\bar{K}]\{x\} = -[M]\{1\}\ddot{x}_g - [K_b]\{d\} \tag{2}$$

where $[\bar{C}], [\bar{K}]$ are equivalent damping matrix and stiffness matrix, respectively. They are defined as

$$[\bar{C}] = [C] + [C_b] \tag{3}$$

$$[\bar{K}] = [K] + [K_b] \tag{4}$$

$$[C_b] = \left[\begin{array}{cc|c} c_b & -c_b & 0 \\ -c_b & c_b & 0 \\ \hline 0 & 0 & 0 \end{array} \right] \quad [K_b] = \left[\begin{array}{cc|c} k_b & -k_b & 0 \\ -k_b & k_b & 0 \\ \hline 0 & 0 & 0 \end{array} \right] \quad \{d\} = \begin{Bmatrix} d \\ 0 \\ \vdots \\ 0 \end{Bmatrix}$$

During right bumping, neglecting the mass of the stopper, the number of degree of freedoms of the system does not increase. The effect of the bumping is to incorporate the restoring force and damping

force of the stopper onto interaction force between mass m_1 and m_2 . The equilibrium equation of the interaction force is

$$c_b \dot{x}_r + k_b x_r = p_{br} \quad (5)$$

where, p_{br} is the force of the isolators applied on the stoppers at the right side. Apparently, we have

$$p_{br} = c_2(\dot{x}_2 - \dot{x}_1) + k_2(x_2 - x_1) \quad (6)$$

In the course of right bumping, i.e. when $p_{br} > 0$, the lateral deformation of the stoppers becomes

$$x_r = x_2 - x_1 - d \quad (7)$$

When $p_{br} = 0$, the isolators and the stoppers separate, and the bumping stops. From this time to the next pounding, the lateral deformation of the stopper complies with the following law (Sun and Goto, 1996)

$$x_r = x_{r0} e^{-\frac{k_b}{c_b}(t-t_{br})} \quad (8)$$

where, x_{r0} is the lateral deformation of the stoppers when the isolators and the stoppers separate.

2.3 Equation of Motion for Left Pounding

When the interstorey displacement of the isolation layer is smaller than the difference of the left stopper deformation and the preset open space, namely, $x_2 - x_1 < x_l - d$, the isolators will pound on the left stoppers. The equation of motion becomes

$$[M]\{\ddot{x}\} + [C]\{\dot{x}\} + [K]\{x\} = -[M]\{1\}\ddot{x}_g + [K_b]\{d\} \quad (9)$$

The notations, involved in the above equation, are same as those in Equation (2). The equation of motion of the left stoppers is

$$c_b \dot{x}_l + k_b x_l = p_{bl} \quad (10)$$

where p_{bl} is the force of the isolators imposed on the stoppers. During the process of left pounding, i.e. $p_{bl} < 0$, the lateral deformation of the stoppers is

$$x_l = x_2 - x_1 + d \quad (11)$$

When $p_{bl} = 0$, the isolators and the left stoppers separate, and the bumping stops. From this moment t_{bl} to next bumping, the lateral deformation of the stoppers is

$$x_l = x_{l0} e^{-\frac{k_b}{c_b}(t-t_{bl})} \quad (12)$$

where x_{l0} is the lateral deformation of the stoppers at time $t = t_{bl}$ when the isolators and the left stoppers separate from each other.

2.4 Solution of the Equations and Computer Code

The motion equations of base-isolated building, with pounding protection of rubber bearings, are solved by Wilson- θ algorithm numerically, the value of θ is chosen as 1.4, and a computer program, incorporating all the possible right and left pounding effects listed in Sub-sections 2.2 and 2.3, has been developed to carry out following analyses. This computer program integrates both the seismic time history analyses of soft pounding system and stiffness variable system. The input data of the program includes structure parameters, ground motion acceleration time history and scale factors, soil property parameters, site category and control variables which are used to fit the different kinds of analysis purposes. The mentioned program, written in FORTRAN language, can be used to analyze shear type non-linear structures by using piecewise linear model (Han, 1997). The outputs of the program include the relative horizontal displacements, interstorey horizontal displacements, shear forces and acceleration responses of superstructure in terms of peak values and time history. The time interval or step in numerical calculations is chosen as 0.02 sec in this study.

3. Numerical Analysis for an Example Building

To demonstrate the effect of soft pounding in aspect of protecting the rubber bearings, we consider a 6-storey building located in seismic zone with ground motion severity of 0.4g. The fundamental period of the fixed-based building is 0.3 sec and that of the base-isolation building is 1.97 sec. We suppose that the structure is located at a site of type III category whose shallow subsoil consists of soft soil layer (clay and sand, the equivalent average shear wave velocity within depth of 20 m is not larger than 140 m/s) and the thickness of overburden is less than 80 m, according to the Chinese seismic design code (CABP, 2001), and assume that the stoppers have been installed in the isolation layer. The analysis model of the structure is same as shown in Figure 2. The parameters of the model are listed as follows. Mass and stiffness of the superstructure: $m_3 = m_4 = m_5 = m_6 = m_7 = 430 \text{ t}$, $m_8 = 270 \text{ t}$, $k_3 = k_4 = k_5 = 2.86 \times 10^6 \text{ kN/m}$, $k_6 = k_7 = k_8 = 2.35 \times 10^6 \text{ kN/m}$. The damping ratio of the superstructure: $\xi' = 0.05$. Mass, stiffness and damping ratio of the isolation layer: $m_2 = 330 \text{ t}$, $k_2 = 2.86 \times 10^6 \text{ kN/m}$, the damping ratio of the isolation layer $\xi'' = 0.05$. Mass of the base: $m_1 = 350 \text{ t}$. Equivalent stiffness and damping coefficient of soil: $k_1 = 5.11 \times 10^6 \text{ kN/m}$, $c_1 = 1.686 \times 10^5 \text{ kN/m}$.

3.1 Pre-option of the Stoppers' Parameters

The preset space d is chosen as 10 cm, 15 cm and 20 cm. The damping coefficient c_b is determined by the value of $CR = c_b/c_2$, where c_2 is damping coefficient of the isolation layer. A set of CR values of 0, 5, 10, 15, 20, 25, 30, 35, 40, 45 and 50 is chosen for comparative analysis. Here, $CR = 0$ means that the damping of the buffer stopper is zero.

The stiffness coefficient, k_b , is determined according to its capacity of recentering TN , which is the ratio of the period of time required by the stopper to recover 10% of the maximum deformation and the fundamental period of the structure. Keep this definition of TN in mind and notice that the frequency of base-isolated building $\omega \cong \sqrt{k_2/M}$, $CR = c_b/c_2$, $t - t_{br} \cong TN \frac{2\pi}{\omega}$ and $\xi'' = \frac{c_2}{2\omega M}$, where $M = \sum_{i=2}^n m_i$.

It is easy to observe from Equation (8) that the following approximate relationship between k_b and k_2 exists

$$\frac{k_b}{k_2} = \frac{-\ln 0.1}{\pi} \cdot \xi'' \cdot CR \cdot \frac{1}{TN} \tag{13}$$

As shown in Equation (13), TN is a parameter related to the flexibility characteristics of the stoppers, the value of which is chosen as 1, 0.5 and 0.25.

3.2 Parameter Option and Optimization for Stoppers

The NS acceleration component of 1940 El Centro earthquake record is used as input motion, but the severity of the recorded motion has been scaled to required design level and then the peak acceleration is chosen 220 gal and 620 gal, which respectively corresponds to the EPA (effective peak acceleration) value of the most probably occurring earthquake and maximum considered earthquake in Chinese seismic design code for buildings. These two levels of design earthquake ground motion, combined with design basis earthquake, whose EPA is 450 gal in this example as mentioned above, form so called multiple level defense provisions in Seismic design code for buildings (CABP, 2001). It is worth pointing out here that the Chinese seismic design code usually requires to only analyze seismic responses of structures subjected to the mentioned most probably occurring earthquake and maximum considered earthquake which also is called extreme earthquake. Using the computer program mentioned in Sub-section 2.4, we calculate the maximum interstorey displacements and maximum interstorey shear forces for input accelerations of 220 gal and 620 gal, and various values of d , CR , TN . The results are listed in Tables 1-4.

The concerned topics in parameter optimization: In aspects of parameter optimum of buffer and restrainer including selection of the stiffness and damping coefficient of the stopper, there are three topics that should be emphasized and each of them provides certain preconditions or requirements to be complied.

Table 1: Maximum Interstorey Displacement D_{2max} (cm) for Model I Subjected to El Centro Record (EPA = 220 gal)

TN	d-CR	0	5	10	15	20	25	30	35	40	45	50
1	10	10.7	10.7	10.6	10.5	10.5	10.4	10.4	10.4	10.4	10.3	10.3
1/2	10	10.7	10.6	10.6	10.5	10.5	10.4	10.4	10.4	10.3	10.3	10.3
1/4	10	10.7	10.6	10.6	10.5	10.4	10.4	10.4	10.3	10.3	10.3	10.3

Table 2: Maximum Interstorey Shear Force Q_{3max} (kN) for Model I Subjected to El Centro Record (EPA = 220 gal)

TN	d-CR	0	5	10	15	20	25	30	35	40	45	50
1	10	2720	3110	3450	3730	3960	4150	4320	4460	4580	4680	4770
1/2	10	2720	3120	3470	3740	3970	4170	4340	4480	4600	4700	4790
1/4	10	2720	3130	3490	3780	4010	4200	4370	4510	4630	4730	4820

Table 3: Maximum Interstorey Displacement D_{2max} (cm) for Model I Subjected to El Centro Record (EPA = 620 gal)

TN	d-CR	0	5	10	15	20	25	30	35	40	45	50
1	10	30.2	22.4	<u>19.3</u>	<u>17.5</u>	16.7	15.8	15.2	14.6	14.3	14.0	13.5
	15	30.2	25.6	23.2	<u>22.0</u>	<u>21.0</u>	20.4	19.9	19.4	19.2	18.8	18.7
	20	30.2	27.9	26.5	25.7	25.0	24.6	24.3	24.1	23.7	23.6	23.4
1/2	10	30.2	<u>21.7</u>	<u>18.6</u>	17.0	16.1	15.3	14.5	14.0	13.6	13.2	13.0
	15	30.2	25.3	22.9	<u>21.7</u>	<u>21.0</u>	20.1	19.8	19.3	19.1	18.6	18.5
	20	30.2	27.7	26.3	25.6	24.9	24.6	24.2	23.8	23.7	23.5	23.1
1/4	10	30.2	<u>21.1</u>	<u>18.2</u>	16.8	15.5	14.7	13.9	13.3	13.0	12.7	12.4
	15	30.2	24.8	22.6	<u>21.4</u>	<u>20.6</u>	20.0	19.4	19.0	18.7	18.4	18.1
	20	30.2	27.5	26.1	25.3	24.7	24.3	23.9	23.7	23.3	23.1	23.0

Table 4: Maximum Interstorey Shear Force Q_{3max} (kN) for Model I Subjected to El Centro Record (EPA = 620 gal)

TN	d-CR	0	5	10	15	20	25	30	35	40	45	50
1	10	7650	7570	<u>9210</u>	<u>10400</u>	11700	12700	13400	13900	14200	14400	15000
	15	7650	8370	10500	<u>12100</u>	<u>13200</u>	14200	15100	15900	16600	17500	18100
	20	7650	8760	10740	12400	13900	15200	16400	17400	18300	19100	19800
1/2	10	7650	<u>7810</u>	<u>9460</u>	10600	12000	12900	13500	13900	14200	14600	15600
	15	7650	8650	10600	<u>12300</u>	<u>13500</u>	14400	15400	16200	16900	17600	18500
	20	7650	8930	10900	12600	14200	15500	16700	17700	18600	19400	20100
1/4	10	7650	<u>8480</u>	<u>10200</u>	11600	12500	13200	13400	13500	14800	15900	17000
	15	7650	9260	11500	<u>13100</u>	<u>14400</u>	15200	15900	16800	17700	18500	19200
	20	7650	9390	11300	13100	14700	16200	17300	18400	19100	19900	20600

- (1) About isolation layer: At first the vertical load and maximum interstorey displacement of isolation layer should be controlled within its allowed values; otherwise the rubber bearings may damage or lose their stability. Based on the related testing results for the prescribed rubber bearings (CABP, 2001; CABR, 1999), the allowed interstorey horizontal displacement of isolation layer D_{2max} for the structure in this example is set as 22 cm if the diameter of the rubber bearings used in isolation layer is 40 cm, and the allowed vertical axis compression stress is 15 MPa.
- (2) Superstructure: The maximum interstorey displacements of the superstructure should be restricted within allowed values stipulated by seismic design code. Meanwhile, the maximum storey shear forces, that usually take place at bottom storey of the superstructure, should be smaller than the allowed value.
- (3) Consideration of construction cost: We should use stoppers as less in size as possible to reduce the cost of construction and maintenance.

Option of parameters

1. *Designed preset space d* : Tables 1 and 2 show that the value of D_{2max} reduces slightly and the value of Q_{3max} increases significantly when increasing the value of CR , which is a parameter depending on damping of the stoppers. For example, when $TN = 1$, and $d = 10$ cm, the value of D_{2max} for $CR = 25$ is 0.3 cm smaller than that for $CR = 0$, the reduction being 2.7%, and the value of Q_{3max} increases from 2720 to 4150 kN, the increase being 52%. Evidently, the disadvantage of the buffer stopper outweighs its advantage during a moderate earthquake of 0.22g. Considering the larger occurrence probability of such kind of a design moderate earthquake in seismic zone of high intensity, the designed preset space should not be too small. We should make sure that the isolators do not bump against the stoppers during a frequently occurring earthquake.

For this example building, the values of D_{2max} just slightly exceed the preset d of 10 cm during the most likely occurrence earthquake with EPA of 0.22g corresponding to the design basic earthquake of 0.45g. So we may choose 10 cm as the lower limit of d value.

As shown in Table 3, when $d = 20$ cm, the inequality, $D_{2max} > 22$ cm, is always satisfied for all the preset values of d . When bumping happens, it is true for all values of d such that $D_{2max} > d$. In order to satisfy the requirement of $D_{2max} < 22$ cm, as mentioned previously, the preset value of d should be less than 20 cm.

2. *The ratio of the damping coefficient of the stoppers and that of isolation layer CR* : From Tables 3 and 4, it can be seen that increasing CR can decrease the value of D_{2max} but the increasing trend of the latter is larger than the reducing trend of the former in case of increased Q_{3max} . So we can determine the lower limit of CR according to condition 1, and the upper limit according to condition 2. Then we give a suitable range for the value of CR , to comply with the requirement 3. In general, the smaller value of CR is preferable from the viewpoint of engineering application. In fact, larger value of CR will create additional difficulty in designing and manufacturing of the stopper. Furthermore, smaller values of CR mean that fewer stoppers are required which is less expensive.

For this building, in consideration of the above three requirements, better values of CR and d can be chosen according to D_{2max} and Q_{3max} as underlined in Tables 3 and 4. For instance, when $d = 10$ cm, $CR = 5-15$ is preferable, and when $d = 15$ cm, $CR = 15-20$ is suitable. Anyway, $d = 15$ cm is more suitable in this case.

3. *Flexible property of the buffer stopper TN* : For a certain value of CR , decreasing TN causes decrease in value of D_{2max} and increase in Q_{3max} . However, the increasing potential of Q_{3max} is over the decreasing one. Thus, the value of TN should not be too small. All the three values of TN , given in Tables 1-4, seem suitable.

Now, let us input Mexico earthquake records of 1985 into the same example structure and make the peak values of acceleration scaled to 220 gal and 620 gal. The maximum interstorey displacements and maximum interstorey shear forces of isolation layer for various values of d , NK and CR are calculated by using the mentioned program and the results are listed in Tables 5-8. Obviously, the input period matches the isolated period in this case and the so called semi-resonance phenomenon takes place. However, the acceleration of the 1985 Mexico record reaches 620 gal nearly which is impossible even for Mexico City. We use it as input motion of the example structure only for numerical comparison's sake. The computation results, shown in Tables 5 and 8, indicate that the maximum interstorey displacement rapidly decreases with increasing CR . However, the changing rule of first interstorey shear force with increasing CR apparently differs from that of interstorey displacement. In fact, the figures, shown in Table 6 and 8, illustrate that the interstorey shear force first decreases and then increases again with increasing CR . If we use rubber bearings of diameter 40 cm, the maximum interstorey displacements, which satisfy the requirement of the lateral deformation of rubber bearing as stipulated in the Chinese seismic design code, and the corresponding shear forces are indicated by the underlined figures in Tables 6 and 8. In consideration of construction feasibility and the general requirement of reducing cost, less

d , CR and larger TN are expected. Thus, $TN = 1$, $d = 10$ cm, and $CR = 20$ is a good choice if input motion EPA = 220 gal. When EPA = 620 gal, only few combinations of d , TN and CR , as indicated by the underlined figures in Tables 7 and 8, enable the maximum displacements of isolation layer less than the allowed value of 22 cm, for example, $d = 10$, $CR = 45$ and $TN = 1$. These results show that by using suitable spring and damper and presetting certain free space between building and stopper in soft pounding system, the lateral displacement of isolation layer can be tremendously reduced within allowed values even though the original displacement of rubber bearings without protection measure is as large as 330 cm. Comparing the computational results listed in Tables 1-8 for Mexico wave and El Centro wave inputs, it can be seen that both displacements of isolation layer and maximum interstorey shear forces decrease simultaneously with increasing CR for Mexico wave, but in contrast, the maximum interstorey shear forces can increase with increasing CR , though the displacements of isolation still decrease for El Centro wave. That means, for El Centro like input wave, the reduction of lateral deformation of base isolation layer is at the cost of increase in shear forces of superstructure. Apparently, the proposed soft pounding protection measure in case of Mexico input is more effective compared to El Centro input.

Table 5: Maximum Interstorey Displacement D_{2max} (cm) for Model I Subjected to Mexico Wave (EPA = 220 gal)

TN	d \ CR	0	5	10	15	20	25	30	35	40	45	50
1	10	117	39.0	29.3	24.1	<u>21.1</u>	<u>19.3</u>	<u>18.0</u>	<u>17.0</u>	<u>16.1</u>	<u>15.7</u>	<u>15.3</u>
	15	117	43.1	34.0	29.2	26.4	24.5	22.9	22.3	<u>21.5</u>	<u>20.9</u>	<u>20.5</u>
	20	117	46.7	38.9	34.3	31.4	29.9	28.4	27.4	26.5	26.1	25.6
1/2	10	117	36.2	26.6	22.0	<u>19.4</u>	<u>17.9</u>	<u>16.6</u>	<u>15.9</u>	<u>15.4</u>	<u>15.1</u>	<u>14.6</u>
	15	117	40.7	31.8	27.4	24.8	23.1	22.1	<u>21.2</u>	<u>20.8</u>	<u>20.3</u>	<u>19.9</u>
	20	117	45.0	37.1	33.0	30.5	28.7	27.7	26.6	26.1	25.6	25.3
1/4	10	117	31.7	23.0	<u>19.2</u>	<u>17.4</u>	<u>16.5</u>	<u>15.7</u>	<u>15.1</u>	<u>14.7</u>	<u>14.4</u>	<u>13.9</u>
	15	117	37.3	28.7	24.9	22.9	<u>21.9</u>	<u>21.1</u>	<u>20.5</u>	<u>20.0</u>	<u>19.6</u>	<u>19.4</u>
	20	117	42.3	34.5	31.0	28.8	27.4	26.5	25.9	25.4	25.0	24.7

Table 6: Maximum Interstorey Shear Force Q_{3max} (kN) for Model I Subjected to Mexico Wave (EPA = 220 gal)

TN	d \ CR	0	5	10	15	20	25	30	35	40	45	50
1	10	29700	12900	13500	14500	<u>15500</u>	<u>16400</u>	<u>17000</u>	<u>17500</u>	<u>18000</u>	<u>18400</u>	<u>18700</u>
	15	29700	14000	15400	16700	17800	18600	19100	19900	<u>20800</u>	<u>21500</u>	<u>22200</u>
	20	29700	14800	17300	18900	20200	21300	22000	22500	23000	23600	24500
1/2	10	29700	13000	13200	14300	<u>15200</u>	<u>16000</u>	<u>16400</u>	<u>17100</u>	<u>17900</u>	<u>18600</u>	<u>19000</u>
	15	29700	14200	15400	16700	17600	18300	19100	<u>20100</u>	<u>21000</u>	<u>21800</u>	<u>22400</u>
	20	29700	15300	17500	19200	20400	21200	21900	22400	23300	24200	24900
1/4	10	29700	13200	13000	<u>13900</u>	<u>15400</u>	<u>16600</u>	<u>17400</u>	<u>18100</u>	<u>18900</u>	<u>19500</u>	<u>19800</u>
	15	29700	14800	15500	16600	17500	<u>19000</u>	<u>20100</u>	<u>21100</u>	<u>21800</u>	<u>22500</u>	<u>23300</u>
	20	29700	16200	18100	19700	20600	21500	22500	23500	24400	25200	25900

Table 7: Maximum Interstorey Displacement D_{2max} (cm) for Model I Subjected to Mexico Wave (EPA = 620 gal)

TN	d \ CR	0	5	10	15	20	25	30	35	40	45	50
1	10	330	97.7	66.4	50.6	41.7	35.8	31.9	28.5	26.4	<u>21.0</u>	23.6
	15	330	101	71.0	56.1	46.5	41.2	36.5	33.6	31.8	30.2	29.0
	20	330	104	75.0	60.3	51.3	46.0	41.7	39.3	37.2	35.6	34.2
1/2	10	330	86.4	56.5	42.4	34.6	30.2	27.1	24.7	23.1	<u>22.0</u>	<u>20.9</u>
	15	330	90.6	61.6	48.1	40.7	35.8	32.5	30.7	29.0	27.7	27.1
	20	330	94.4	66.6	53.6	45.8	41.0	38.0	36.4	34.7	33.3	32.9
1/4	10	330	70.8	44.2	33.5	28.6	25.5	23.4	<u>21.7</u>	<u>20.7</u>	<u>19.7</u>	<u>18.8</u>
	15	330	76.1	50.6	39.2	34.7	31.7	29.4	28.1	26.8	25.7	25.2
	20	330	81.0	55.8	45.3	40.1	37.2	35.4	34.2	32.8	31.7	30.8

Table 8: Maximum Interstorey Shear Force Q_{3max} (kN) for Model I Subjected to Mexico Wave (EPA = 620 gal)

TN	d CR	0	5	10	15	20	25	30	35	40	45	50
1	10	83600	32600	31200	33000	34600	35900	37388	38100	39400	<u>40500</u>	41400
	15	83600	33600	33200	35800	37300	39300	40300	41700	43200	44400	45600
	20	83600	34600	34900	37700	39800	41900	43400	45100	46500	47700	48700
1/2	10	83600	32000	29000	30100	31400	33100	34300	35400	37000	<u>38200</u>	<u>38700</u>
	15	83600	33300	31500	33500	35500	37000	38400	40000	41500	42800	44700
	20	83600	34400	33600	36400	38300	40100	41700	43900	45600	47100	49200
1/4	10	83600	31400	27500	27100	29300	31800	34000	<u>35400</u>	<u>37300</u>	<u>38300</u>	<u>39200</u>
	15	83600	33200	30000	31100	34300	37300	39300	41800	43300	44500	46600
	20	83600	34600	32500	35100	37500	40800	43800	46600	48300	49900	51200

Now, let us move to maximum absolute acceleration responses for model I, for instance on taking $TN = 1$ and $d = 10$ cm. The distribution of peak acceleration along height of the building is shown in Table 9, in which n represents the floor number of the example building. When $CR = 0$, that means no protection measure is adopted in the structure, the absolute acceleration responses are slightly increased along height but their diversification along height or floor levels is very small. It can be seen from Table 9 that the absolute peak acceleration increases with increasing CR and decreasing floor number n , and the maximum value usually is located at third floor level, next to isolation layer. The amplification of acceleration at the third floor level with increasing CR usually comes from high frequency shock in the pounding process. If CR is approaching to infinity, or TN approaching to zero, as indicated by Equation (13), which shows the relation between CR and TN , the behavior of the system closes to hard pounding without buffer. Thus, the absolute accelerations are gradually amplified and the distribution of acceleration along height turns from inclined straight line to K shape line as can be seen in Table 9. Hard pounding surely is harmful to the superstructure. Anyway, appropriate incorporating springs and buffers are able to eliminate high frequency vibrations induced by the hard pounding.

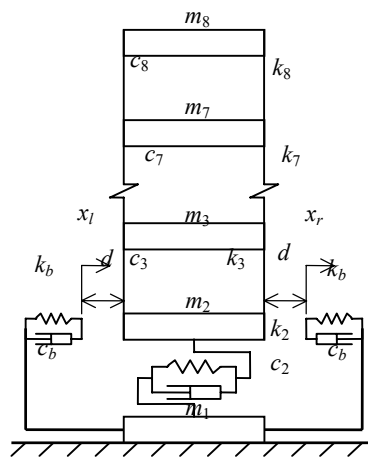


Fig. 3 Mechanical model (II)

4. Simplified Analysis of Base-isolated Building on Rigid Foundation

For base-isolated building on rigid foundation, the model I can be simplified as model II (see Figure 3), in which the soil-structure interaction is neglected. Therefore, mass m_1 and the stopper are fixed and the 8-DOF system is reduced to a 7-DOF system.

In model II, all the parameters are same as in model I except mass m_1 which is vanished in this case. The same analysis method has been used to calculate the seismic responses as for model I. It should be noted that, in this case, the first several natural periods of the base isolation system without considering the effect of soil-structure interaction are almost same as the corresponding values of the structure with interaction effects. Parts of the results for the base isolation building on rigid foundation are listed in Tables 10-11. Comparing the results of Tables 10 and 3, 11 and 4, it is found that the differences among

them are very small which means that for this example structure, the effects of soil-structure interaction can be neglected. Therefore, we can use model II instead of model I to analyze the example building. For this reason, only cases without consideration of interaction effects are discussed in following sections.

Table 9: Maximum Absolute Acceleration (cm/s²) for Model I Subjected to El Centro Wave (EPA = 620 gal)

<i>TN</i>	<i>D</i>	<i>n CR</i>	0	5	10	30	50	100	Hard Pounding
1	10	3	312	540	814	1469	1770	2878	5750
		4	315	452	644	1108	1288	2050	4510
		5	316	422	591	988	1119	1730	3780
		6	318	405	552	887	1049	1550	3070
		7	319	474	646	1038	1210	1880	3700
		8	319	555	778	1281	1490	2370	4860

Table 10: Maximum Interstorey Displacement D_{2max} (cm) for Model II Subjected to El Centro Wave (EPA = 620 gal)

<i>TN</i>	<i>d CR</i>	0	5	10	15	20	25	30	35	40	45	50
1	10	30.1	224	<u>19.3</u>	<u>17.6</u>	<u>16.6</u>	<u>15.8</u>	<u>15.3</u>	<u>14.7</u>	<u>14.2</u>	<u>14.0</u>	<u>13.6</u>
	15	30.1	25.6	23.3	21.9	21.0	20.4	<u>19.9</u>	<u>19.6</u>	19.2	19.0	18.6
	20	30.1	27.7	26.5	25.7	25.1	24.7	24.3	24.1	23.8	23.6	23.4
1/2	10	30.1	21.7	<u>18.7</u>	<u>17.1</u>	<u>16.1</u>	<u>15.3</u>	<u>14.6</u>	<u>14.0</u>	<u>13.5</u>	<u>13.2</u>	<u>13.1</u>
	15	30.1	25.3	23.0	21.7	21.0	20.3	<u>19.8</u>	<u>19.3</u>	19.0	18.81	18.4
	20	30.1	27.7	26.3	25.6	25.0	24.6	24.2	23.9	23.7	23.5	23.3
1/4	10	30.1	21.1	<u>18.3</u>	<u>16.6</u>	<u>15.5</u>	<u>14.5</u>	<u>13.9</u>	<u>13.3</u>	<u>13.0</u>	12.7	12.4
	15	30.1	24.8	22.6	21.4	20.6	<u>20.0</u>	<u>19.4</u>	19.0	18.7	18.4	18.2
	20	30.1	27.5	26.2	25.3	24.7	24.3	24.0	23.6	23.4	23.2	23.0

Table 11: Maximum Interstorey Shear Force Q_{3max} (kN) for Mode II Subjected to El Centro Wave (EPA = 620 gal)

<i>TN</i>	<i>d CR</i>	0	5	10	15	20	25	30	35	40	45	50
1	10	7630	7590	<u>9240</u>	<u>10670</u>	<u>12000</u>	<u>13100</u>	<u>13800</u>	<u>14300</u>	<u>14700</u>	<u>15100</u>	<u>16000</u>
	15	7630	8390	10600	12300	13600	14700	<u>15600</u>	<u>16500</u>	17300	18100	18800
	20	7630	8770	10900	12700	14300	15700	17000	18100	19100	20000	20700
1/2	10	7630	7850	<u>9510</u>	<u>11000</u>	<u>12400</u>	<u>13400</u>	<u>14000</u>	<u>14400</u>	<u>14700</u>	<u>15700</u>	<u>17000</u>
	15	7630	8670	10700	12300	13800	14900	<u>15900</u>	<u>16800</u>	17700	18500	19200
	20	7630	8930	11000	12898	14543	16006	17300	18433	19400	20303	21000
1/4	10	7630	8510	<u>10300</u>	<u>11600</u>	<u>12800</u>	<u>13500</u>	<u>13900</u>	<u>14500</u>	<u>15900</u>	17200	18400
	15	7630	9300	11500	13200	14400	<u>15500</u>	<u>16500</u>	17500	18400	19200	20100
	20	7630	9400	11400	13400	15200	16700	18000	19000	20000	20800	21600

Unlike hard impact between building and moat wall, we did not observe apparent harmful high frequency components in this example structure, either incorporating soil-structure interaction or not, when some dampers are equipped together with springs in parallel as shown in Figures 2 and 3. This is an advantage of soft pounding system over hard pounding.

STIFFNESS-VARIABLE PROTECTION SYSTEMS

1. Fundamental Principle

The primary idea of stiffness variable protection comes from observation of displacement response spectra which give the relationship between the peak displacement and the natural period of SDOF oscillator with certain damping. In fact, the smoothed displacement response spectra calculated from variety of acceleration records have common tendency of increase with increasing period. Based on this idea, a stiffness variable protection system has emerged in which an additional stiffness component is

equipped at abutments certain distance away from the protected rubber bearings, with substituting additional stiffness components acting as stiffness regulator. The relationship between restoring force and displacement of isolation layer equipped with supplemental springs is shown in Figure 4 in which K is initial stiffness of isolation layer or sum of stiffnesses of all the rubber bearings placed in the isolation layer and K_b is stiffness of the supplemental spring. Once the lateral displacement of the isolation layer reaches d , as shown in Figure 4, the supplemental spring is permanently tied up to rubber bearings in the isolation layer and then the total stiffness of the isolation layer becomes K_b+K (see Figure 4). If the displacement of rubber bearing, which usually is caused by somewhat resonance effect from long period ground motions, is too large and reaches the prescribed limitation, the additional stiffness components will work together with rubber bearings. Then, the possibility of further increase of the displacement of rubber bearings would be suppressed because the natural period of the base-isolated building has been changed.

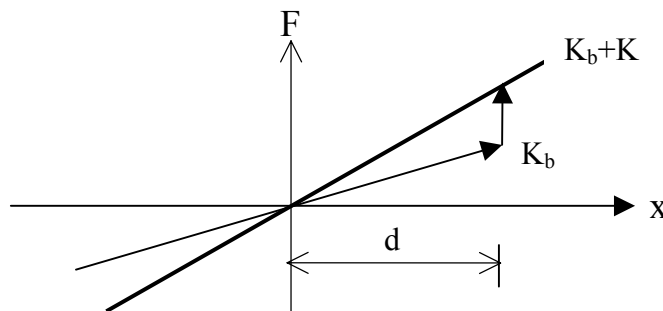


Fig. 4 The relation between force-displacement

2. Mechanical Model and Equations of Motion

The mechanical model of base-isolated buildings and equations of motion under earthquake excitation has close similarity compared with soft pounding system described in preceding sections and only slight change is necessary in this case as depicted in following paragraphs. On this supposition, if using rigid foundation, the mechanical model will be similar as shown in Figure 3 but $c_b = 0$ without rebound in this case.

2.1 Equations of Motion without Additional Stiffness Component

When $-d \leq x_2 \leq d$, additional stiffness component has no effects on the motion of the structure. The model, in Figure 3, becomes a common shear structure, the equation of motion is the same as Equation (1), but the number of degree-of-freedom reduces to $n - 1$.

2.2 Equations System of Motion with Supplemental Stiffness Device

If the supplemental spring is installed only at the right side of the building and $x_2 > d$, i.e. the displacement of the isolation layer is larger than the preset open space d on the right side, the isolators will bump against the additional stiffness device. The stiffness of the isolation layer will increase k_b . The equations of motion after pounding are given by

$$[M]\{\ddot{x}\} + [C]\{\dot{x}\} + [\bar{K}]\{x\} = -[M]\{1\}\ddot{x}_g + [K_b]\{d\} \tag{14}$$

where $[\bar{K}]$ is equivalent stiffness matrix and is the same as Equation (4), but

$$[K_b] = \begin{bmatrix} k_b & | & 0 \\ \hline 0 & | & 0 \end{bmatrix} \tag{15}$$

The meanings of the notations in the above equations are identical with those of the preceding equations.

In contrast, if the supplemental spring is installed only at the left side and $x_2 < -d$, the isolators will bump against the left additional stiffness device. The equations of motion after pounding are just the same as the mentioned right pounding. It should be noted that once the bump occurs, the additional spring is

tightly connected with the base-isolated building and is no longer separated afterwards. This is the difference between soft pounding protection and stiffness variable protection although they both have preset free space between building and protection devices. However, the supplemental spring can be installed either at the right side or the left side and both sides as well.

3. Analysis for an Example Building

Here, the preceding example building (model II) is considered. The period of the isolated structure is still retained at 1.97 sec in model II without soil-structure interaction. In order to discuss the parameter optimization for the systems of stiffness variable protection, we suppose that the systems of stiffness variable protection have been installed in the isolation layer.

The preset space d is chosen as 6 cm, 8 cm, 10 cm and 12 cm. The stiffness coefficient k_b is determined by the value of $NK = k_b/k_2$, where k_2 is stiffness coefficient of the isolation layer. The value of the NK is chosen as 0, 0.5, 1.0, 2.0 and 4.0. None of the protection devices means $NK = 0$. The relationship between NK and TN is $NK \cdot TN = \frac{-\ln 0.1}{\pi} \cdot \xi^n \cdot CR$ according to Equation (13).

In this sub-section, the Mexico earthquake record of 1985 is first used as input motion and the peak values for both the acceleration records are scaled to 220 gal and 620 gal (corresponding to elastic design earthquake and maximum considered earthquake in the seismic design code of China). The maximum interstorey displacements and maximum interstorey shear forces of isolation layer under excitation of Mexico records, for various values of d and NK , are calculated by using the program mentioned earlier and the results are listed in Tables 12-15. Obviously, the input period matches natural period of the seismically isolated building and the phenomena like resonance-response would happen in the base-isolated structure. If we select rubber bearing of 40 cm in diameter, whose allowable displacement is 22 cm according to the Chinese technology standard of base isolation rubber bearing, and without stiffness variable protection, this example structure would fail when it is subjected to Mexico wave even when the input peak acceleration is only 220 gal. This is because the interstorey displacement of isolation layer, D_{\max} , is 117 cm much larger than the allowed one. In fact, in this particular case, adopting base isolation scheme is not a good option either from economical or technical viewpoint. However, the occurrence probability of long period ground motion like Mexico wave is very small for most of earthquake prone areas except Mexico City. In order to deal with such kind of small probability event, stiffness variable protection system is a good choice. Actually the results shown in Tables 12 and 14 indicate that the first interstorey displacement rapidly decreases with increasing NK , the stiffness ratio of additional springs and rubber bearings. It can be seen from Table 12 that the first interstorey displacement, $D_{2\max}$, slightly increases with increasing preset open space d in case of EPA = 220 gal. However, when EPA reaches 620 gal, $D_{2\max}$ seems no longer dependent on d in spite of what CN values are as shown in Table 14. As for the influence of d on first interstorey shear force, the situation is little bit complex. Generally speaking, the shear force increases with increasing d (see Table 13) but when EPA = 620 gal, the amplitudes of increase become very small (see Table 15). Furthermore, the figures shown in Table 13 indicate that the first storey shear forces first decrease and reach their minimum values at some points within $NK = 1-2$ and then increase with increasing NK . When EPA reaches 620 gal, both the first storey displacements and shear forces monotonically decrease with increasing NK and the influence of d value is quite small as illustrated in Tables 14 and 15. The computational results in Tables 12 and 13 illustrate that $NK = 2$ and small d value, for instance $d = 6$ cm, would be better choice when EPA reaches 220. The underlined figures in Tables 12-15 represent the allowed values of maximum displacements and corresponding shear forces. These underlined figures indicate that in case of EPA = 620 gal, NK should be taken 4 to fit the requirement of seismic design code and that the influences of d either on displacement of isolation layer or on maximum structure shear force are insensitive. As mentioned previously, the situation of EPA reaching 620 gal is almost impossible even at Mexico City if the dominant period of ground acceleration is retained at 2.5 sec. We considered this particular case only for numerical comparison with other cases.

Now let us look at the results of analysis when the base isolation building is subjected to the El Centro wave (see Tables 16-19). In this case, the maximum displacements of seismic isolation layer exceed allowable value of 22 cm only when EPA is larger than 620 gal. When the input peak acceleration equals 220 gal, the stiffness variable system with $d = 5-12$ cm and $NK = 0.5-4$ almost has no effect on

the first interstorey displacement or lateral deformation of isolation D_{2max} as shown in Table 16. In fact, the figures listed in the column of $NK = 0$ and the row of $d = 12$ cm indicate the displacement of isolation layer of the building without stiffness variable spring, i.e. 10.7 cm, which has only tiny difference compared with all the other figures in Table 16. As for shear forces, it seems unfavorable if adopting stiffness variable protection in case of EPA = 220 gal. Actually, unlike Mexico wave input, the shear forces of the seismic isolation layer of the example building always increase with increasing NK values as shown in Tables 17 and 19. When EPA = 620 gal, the first interstorey displacement has minimum value in the vicinity of $NK = 1$, and the first interstorey displacement increases within $NK = 1.0-4.0$ under El Centro wave excitation as shown in Table 18. This is because the period of base-isolated building is approaching the period of input motion with NK increasing from 1 to 4. Therefore, $NK = 0.5-2$ and $d = 6-10$ cm seem more reasonable options. It seems unnecessary to use stiffness variable system when the effective peak acceleration EPA = 220 gal but the safety of superstructure and rubber bearings cannot get insurance when EPA = 620 gal since the earthquake intensity is too large if using rubber bearings of diameter 40 cm. In order to protect superstructure and rubber bearings in isolation layer concerning both the input waves, adopting rubber bearings of 40 cm in diameter, accompanied by stiffness variable system of $NK = 0.5-1$ and $d = 10-12$, seems a reasonable option in this example.

Table 12: Maximum Interstorey Displacement D_{2max} (cm) for Model II Subjected to Mexico Wave (EPA = 220 gal)

$d \backslash NK$	0	0.5	1	2	4
6	117	40.5	23.9	<u>12.7</u>	<u>7.75</u>
8	117	41.7	25.8	<u>17.6</u>	<u>15.2</u>
10	117	41.7	26.2	<u>18.4</u>	<u>15.2</u>
12	117	41.8	26.9	<u>19.5</u>	<u>15.9</u>

Table 13: Maximum Interstorey Shear Force Q_{3max} (kN) for Model II Subjected to Mexico Wave (EPA = 220 gal)

$d \backslash NK$	0	0.5	1	2	4
6	29700	15400	12000	9640	9820
8	29700	15800	13100	<u>13700</u>	<u>17400</u>
10	29700	15800	13300	<u>14200</u>	<u>19000</u>
12	29700	15800	13600	<u>14800</u>	<u>20900</u>

Table 14: Maximum Interstorey Displacement D_{2max} (cm) for Model II Subjected to Mexico Wave (EPA = 620 gal)

$d \backslash NK$	0	0.5	1	2	4
6	330	114	66.3	34.3	<u>19.6</u>
8	330	114	66.5	34.6	<u>19.9</u>
10	330	114	66.6	34.6	<u>20.2</u>
12	330	114	66.7	34.9	<u>20.6</u>

Table 15: Maximum Interstorey Shear Force Q_{3max} (kN) for Model II Subjected to Mexico Wave (EPA = 620 gal)

$d \backslash NK$	0	0.5	1	2	4
6	83600	43410	33600	26000	<u>24800</u>
8	83600	43400	33600	26100	<u>25100</u>
10	83600	43400	33700	26300	<u>25500</u>
12	83600	43400	33700	26500	<u>26100</u>

The figures shown in Tables 12-19 also indicate that when $NK = 0$, which is the case of normal base isolation system without supplemental spring, the preset space d is meaningless because it does not impart any influence either on interstorey displacements or on shear forces. Furthermore, if the preset space d is larger than the maximum response of the isolation layer, installation of supplemental spring is meaningless because it never takes part in any work during the earthquake. Similar situation can be expected for the previously discussed soft pounding protection system. From this point of view, both the protection systems of soft pounding and variable stiffness have similar characteristics.

Table 16: Maximum Interstorey Displacement D_{2max} (cm) for Model II Subjected to El Centro Wave (EPA = 220 gal)

$d \backslash NK$	0	0.5	1	2	4
6	10.7	9.60	9.60	9.60	9.60
8	10.7	9.88	9.60	9.60	9.60
10	10.7	10.4	10.2	10.1	10.1
12	10.7	10.7	10.7	10.7	10.7

Table 17: Maximum Interstorey Shear Force Q_{3max} (kN) for Model II Subjected to Input El Centro Wave (EPA = 220 gal)

$d \backslash NK$	0	0.5	1	2	4
6	272	361	438	609	934
8	272	382	492	718	1170
10	272	416	561	845	1390
12	272	272	272	272	272

Table 18: Maximum Interstorey Displacement D_{2max} (cm) for Model II Subjected to Input El Centro Wave (EPA = 620 gal)

$d \backslash NK$	0	0.5	1	2	4
6	30.2	22.52	<u>17.1</u>	23.4	29.4
8	30.2	22.3	<u>17.7</u>	22.5	30.0
10	30.2	22.1	<u>18.3</u>	<u>21.5</u>	30.0
12	30.2	<u>21.8</u>	<u>18.9</u>	<u>20.5</u>	29.3

Table 19: Maximum Interstorey Shear Force Q_{3max} (kN) for Model II Subjected to Input El Centro Wave (EPA = 620 gal)

$d \backslash NK$	0	0.5	1	2	4
6	7660	8540	<u>8690</u>	17800	37400
8	7660	8480	<u>8980</u>	17200	38200
10	7660	8390	<u>9300</u>	<u>16400</u>	38100
12	7660	<u>8280</u>	<u>9600</u>	<u>15600</u>	37300

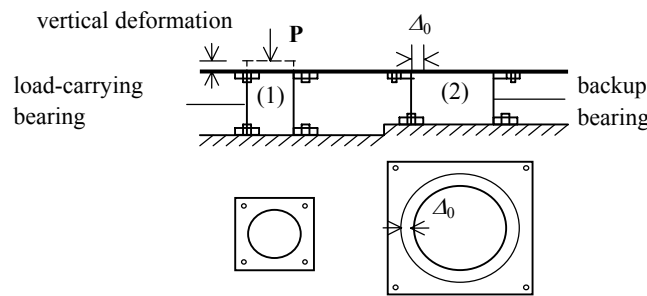


Fig. 5 Schematic model of parallel system

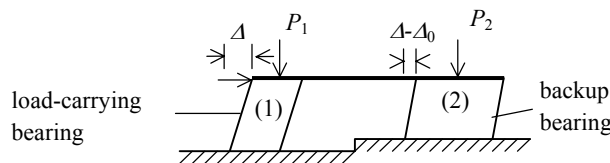


Fig. 6 Lateral displacement of the parallel system

SOFT LANDING PROTECTION

1. Fundamental Principle

The concept of soft landing protection was first presented and tested by Kelly et al. (1980). To illustrate the soft landing protection of the isolation bearing, consider the parallel isolation system as shown in Figure 5. The system consists of two rubber bearings topped by a rigid platform (floor). The big bearing is installed after the small one has ended its vertical deformation. The small bearing carries the entire vertical load of the superstructure, so we call it original load-carrying bearing. The big one bears no vertical load in static state and is called backup bearing. It needs to be noted that the small bearing and the big one in Figure 5 represent all of load-carrying bearings and backup bearing in isolation layer, respectively. Assume that two ends of the bearings are connected with beams (upper beam and lower beam) by steel rings or round loops. The diameters of all the steel round loops surrounding load carrying and backup bearings are the same as those of the bearings except the upper steel loop of the backup bearing, whose diameter is $2\Delta_0$ larger than that of the backup bearing as shown in Figure 5. When the upper beam moves against the lower beam, slippage would be taking place between the top surface of the backup bearing and the lower one of the upper beam. Suppose that the friction coefficient between the two slipping surfaces is μ . As mentioned previously, the axial force of the backup bearing is zero, thus, the original frictional force is zero too.

To analyze the process of the transmission of axial force, the following simplified assumptions are made:

1. The force-displacement relations of the load-carrying bearing and backup bearing are coincided to comply with the assumption of elastic deformation, and k_{v1} and k_{v2} are their vertical stiffness coefficients, respectively.
2. Assume that two ends of the two bearings can only move translationally when analyzing their lateral deformations. The horizontal stiffness is determined according to the approximate theory proposed by Gent (1964), including the effect of flexural deformations and axial force ($P-\Delta$ effect).
3. The bearings' subsidence displacement caused by large horizontal displacement is determined by the approximate method proposed by Kelly (1998). Thus, the additional vertical displacement, δ_v , is given by

$$\delta_v = \frac{P\Delta^2}{P_{cr}\sqrt{2\pi rS}} \tag{16}$$

where P_{cr} is the critical force of the bearing, whose value can be calculated by using a well known formula (Gent, 1964; Koh and Kelly, 1986; Zhou et al., 1997; Zhou et al., 2000), r is the radius of bearings, and S is the first shape coefficient, for cylinder bearing, $S = r/2t_r$, in which t_r is the thickness of the laminated rubber.

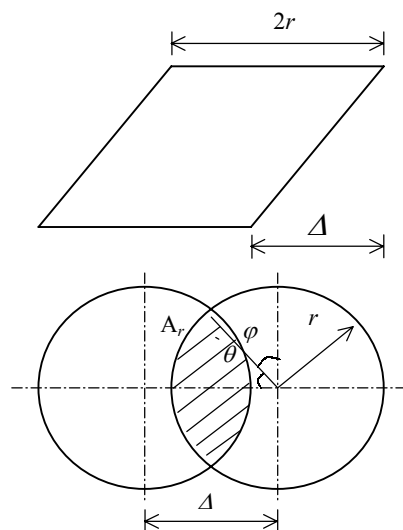


Fig. 7 Rubber bearing in large horizontal deformation

Given above assumptions, when the horizontal displacement of the system is larger than the value of Δ_0 , the horizontal deformations of the two bearings are Δ and $\Delta - \Delta_0$, respectively (see Figure 6). During the course of deformation, a part of the axial force of the load-carrying bearing is transferred to the backup bearings.

According to the consistency condition of vertical deformations (see Figures 5 and 6), we have

$$-\frac{(P - P_1)}{K_{v1}} + \delta_{v1} = \frac{P_2}{K_{v2}} + \delta_{v2} \quad (17)$$

where P_1 , P_2 , K_{v1} , K_{v2} are axial force and vertically compression coefficient of the bearing 1 and bearing 2, respectively; δ_{v1} and δ_{v2} are the additional vertical displacements of the bearing 1 and bearing 2 due to horizontal displacement. It can be found that the following equations are true:

$$P = P_1 + P_2 \quad (18)$$

$$\delta_{v1} = c_1 \Delta^2 \quad (19)$$

$$\delta_{v2} = c_2 (\Delta - \Delta_0)^2 \quad (20)$$

where

$$c_1 = \frac{P_1}{p_{1cr} \sqrt{2\pi r_1 S_1}}; \quad c_2 = \frac{P_2}{p_{2cv} \sqrt{2\pi r_2 S_2}}$$

Substituting Equations (18), (19) and (20) into Equation (17) and rearranging it, following equation is obtained

$$\frac{P_1}{P} = \frac{1 + \left[\frac{1}{K_{v2}} + \frac{(\Delta - \Delta_0)^2}{\sqrt{2\pi r_2 S_2 P_{2cr}}} \right] K_{v1}}{1 + \left[\frac{1}{K_{v2}} + \frac{(\Delta - \Delta_0)^2}{\sqrt{2\pi r_2 S_2 P_{2cr}}} + \frac{\Delta^2}{\sqrt{2\pi r_1 S_1 P_{1cr}}} \right] K_{v1}} \quad (21)$$

Through solving Equations (21) and (18), one obtains the axial force of the two bearings. When $\Delta \leq \Delta_0$, Equation (21) can be simplified as

$$\frac{P_1}{P} = \frac{1 + \frac{K_{v1}}{K_{v2}}}{1 + \frac{K_{v1}}{K_{v2}} + \frac{\Delta^2 K_{v1}}{\sqrt{2\pi r_1 S_1 P_{1cr}}}} \quad (22)$$

Notice that Equation (22) is true for $\Delta_0 = 0$, i.e. there is no free space between the backup bearing and its upper steel loop. When the backup is rigid, obviously, $K_{v2} = \infty$, $P_{2cr} = \infty$ in Equations (21) and (22).

It needs to be noted that the horizontal displacement of the backup bearing caused by frictional force (μP_2) is neglected. In fact, when the value of Δ_0 is small, the values of P_2 and μP_2 are small too. In addition, the effect of the large horizontal displacement on critical force is neglected. This factor, however, is relatively more important and will be discussed in next section.

2. Effect of Large Horizontal Displacement on Critical Force and Distribution of Axial Force

To simplify the problem, the critical force is determined by the following equation (Kelly, 1998; Zhou et al., 1997)

$$P_{cr} = \sqrt{GA EI} \frac{\pi}{h} \quad (23)$$

where G is equivalent shear modulus, E is equivalent Young's modulus of rubber bearing, I is second moment of cross-section, A is the net area of the section (the area of interior steel plate), and h is the

height of the bearing (not including the two end steel plates). Equation (23) is deduced according to the theory of bending-shear beam, which chiefly undertakes shear deformation only while comprising small bending deflection. In case of large deformations, the bearing will deform as shown in Figure 7, where the effective load-bearing area, A_r , is the shadowy area, the crossing part of the two circles in Figure 7. Let α be the ratio of load-bearing area, A_r , and the area of section A , then we have

$$A_r = \alpha A \tag{24}$$

It is easy to find the relation between α and Δ from Figure 6. Kelly (1998) used Taylor's series expansion, neglecting the high order terms, to obtain the following equations

$$\alpha = 1 - \frac{4\lambda}{\pi} + \frac{2}{3\pi}\lambda^3 + \frac{\lambda^5}{10\pi} \quad (\lambda < 0.8) \tag{25}$$

$$\alpha = \frac{8\sqrt{2}}{3\pi}(1-\lambda)^{3/2} \quad (0.8 \leq \lambda < 1) \tag{26}$$

where, λ is the ratio of horizontal displacement and the diameter of the bearing, i.e. $\lambda = \Delta/2r$.

In Equation (23), on substituting A_r for A , we can get the equation of the critical force

$$p'_{cr} = \sqrt{\alpha GAEI} \frac{\pi}{h} = \sqrt{\alpha} p_{cr} \tag{27}$$

After including the effects of the large deformations, Equation (21) can be rewritten as

$$\frac{P_1}{P} = \frac{\frac{1}{K_{V1}} + \frac{1}{K_{V2}} + \beta}{\frac{1}{K_{V1}} + \frac{1}{K_{V2}} + \alpha + \beta} \tag{28}$$

where, α, β are given by following equations:

1. When $0 < \Delta < 1.6r_1$,

$$\alpha = \frac{\Delta^2}{\sqrt{2\pi r_1 s_1} [1 - \frac{2\Delta}{\pi r_1} + \frac{1}{12\pi} (\frac{\Delta}{r_1})^3 + \frac{1}{320\pi} (\frac{\Delta}{r_1})^5]^{1/2} P_{1cr}} \tag{29}$$

When $1.6r_1 \leq \Delta < 2r_1$,

$$\alpha = \frac{\Delta^2}{\frac{16}{3} r_1 s_1 (1 - \frac{\Delta}{2r_1})^{3/4} P_{1cr}} \tag{30}$$

2. When $0 < \Delta \leq \Delta_0$, $\beta = 0$.

When $0 < \Delta - \Delta_0 < 1.6r_2$,

$$\beta = \frac{(\Delta - \Delta_0)^2}{\sqrt{2\pi r_2 s_2} [1 - \frac{2(\Delta - \Delta_0)}{\pi r_2} + \frac{1}{12\pi} (\frac{\Delta - \Delta_0}{r_2})^3 + \frac{1}{320\pi} (\frac{\Delta - \Delta_0}{r_2})^5]^{1/2} P_{2cr}} \tag{31}$$

When $1.6r_2 \leq \Delta - \Delta_0 < 2r_1$,

$$\beta = \frac{(\Delta - \Delta_0)^2}{\frac{16}{3} r_2 s_2 (1 - \frac{\Delta - \Delta_0}{2r_2})^{3/4} P_{2cr}} \tag{32}$$

When the backup bearing is assumed to be a rigid bearing, the distribution of the total vertical load between loading and backup bearing still can be calculated by Equations (28) to (32), but in this case, $K_{V2} = \infty, P_{2cr} = \infty$.

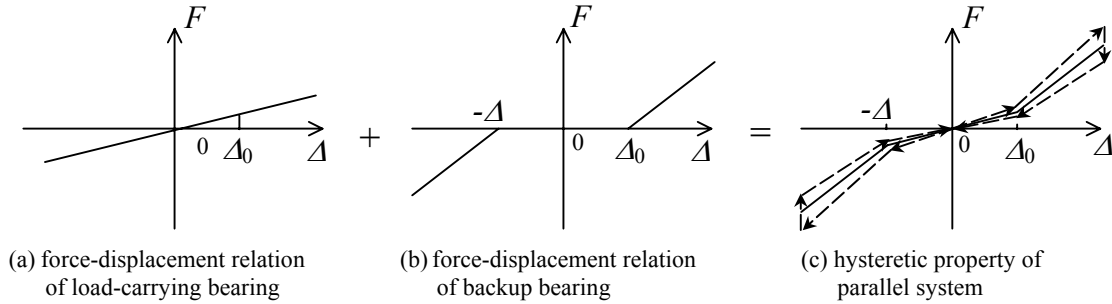


Fig. 8 Horizontal stiffness property of parallel system

3. Relation of Force-Displacement of the Parallel System

The parallel system shown in Figure 5 has force-displacement behavior as illustrated in Figure 8. Here, the solid line represents the skeleton curve neglecting the effect of frictional force and hysteretic loop. As illustrated in Figure 8, when $\Delta < \Delta_0$, the stiffness of the system is the same as that of the load-carrying bearing K_{H1} . On including the effect of large displacement on critical force, it is given by

$$K_{H1} = \frac{G_1 A_1}{h_1} \left(1 - \frac{P_1^2}{\alpha_1 P_{1cr}^2}\right) \tag{33}$$

where the subscript 1 represents bearing 1, and other notations are the same as previously mentioned. The value of Δ increases as horizontal force increases. When $\Delta \geq \Delta_0$, bearings 1 and 2 get compressed and subside down slightly and some horizontal force begins to transfer to bearing 2. In this case, the stiffness of the system, K_H , becomes

$$K_H = K_{H1} + K_{H2} \tag{34}$$

K_{H2} can be determined by Equation (33), just by substituting subscript 2 for 1. When it happens, the horizontal stiffness of the backup bearing will reduce the horizontal displacement. Then, the transferring of the axial force can protect the load-carrying bearing from losing its stability. Considering the above advantage of this system, the load-carrying bearing does not need to satisfy the provision of $\Delta \leq 1.1r_1$, which is a general requirement for base-isolation system in the seismic design code of China (CABP, 2001). This requirement means that the allowed maximum displacement of a rubber bearing cannot exceed 55% of the diameter of the rubber bearing. The code also requires that $\Delta \leq 3.0h_r \times n$ (where h_r is the thickness of each rubber layer and n is the total number of rubber layers). In fact, the results of the lateral deformation capacity tests for base isolation rubber bearings subjected to horizontal shear force under allowed vertical loading condition show that both of the requirements should be satisfied. Otherwise, the load-carrying bearing might lose its loading capacity. In this system, even if the load-carrying bearing fails, the system will remain safe and will continue to withstand the dead load and lateral force until the backup bearing fails.

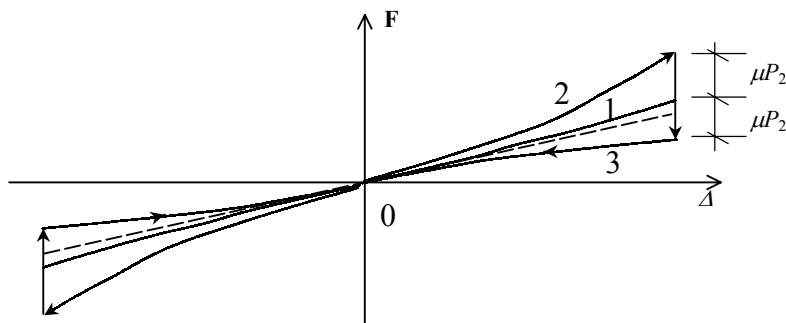


Fig. 9 Hysteretic property of parallel system with rigid backup bearing

Suppose that the frictional coefficient of the sliding surface of the backup bearing is μ , then the frictional force is μP_2 . The values of P_2 and μP_2 increase with an increase in the horizontal displacement. Thus, the actual force-displacement behavior of the system is as shown in dashed line in Figure 8(c). When the system is subjected to cyclic horizontal load, its force-displacement behavior becomes a hysteretic loop. Notice that the values of P_2 and μP_2 are negligible when the value of Δ is small.

However, using large diameter rubber bearing as backup bearing will lead to more cost. In case of large deformations, the backup bearing is required to carry all of the vertical load and the horizontal force transmitted from the top slippage plate, but there is no special requirement for its horizontal deformation capacity. To reduce the cost of seismic design, we can use rigid bearings, such as infilled-concrete steel tube abutments, instead of rubber bearings. Let the frictional coefficient of its upper sliding surface be μ . Then, the force-displacement relation of the system is as shown in Figure 9. Here, the dashed line represents the force-displacement behavior of load-carrying bearings under force P . Curve 1 represents that of the parallel system while including the reducing effect of the force on the load-carrying bearing with increase in the horizontal displacement. Curve 2 represents that of the system when including the effect of frictional force. Curve 3 represents that of the system unloading. The area of the hysteretic loop consisting of curve 2 and curve 3 is the dissipating energy of the system under half-cycle load. In the system mentioned above, the value of second shape coefficient of the load-carrying bearings can be relatively large, i.e. smaller and higher rubber bearings can be used. The provision $\Delta \leq 1.1r_1$ needs not be satisfied. Thus, even for small size building, the fundamental period of base-isolated structure can be relatively longer, for instance 3.0 sec or 4.0 sec. In addition, the frictional force of the backup bearing increases with the increasing of the displacement, hence, this system is actually a variable friction system; the increasing frictional force can effectively restrict the maximum displacement of the load-carrying bearing. The other advantage of this system is that a relatively large frictional coefficient can be chosen, and then cheaper frictional material is available.

4. Numerical Example

To illustrate the effectiveness of above parallel systems, we consider a system consisting of the load-carrying bearings and the backup bearings. The backup bearings are rubber bearings or rigid abutments and pairs.

The parameters of the load-carrying bearings are: diameter $d = 300$ mm, thickness of laminated rubber $t_r = 5.0$ mm, number of layers of the bearing $n = 12$, thickness of the laminated steel plate $t_s = 1.5$ mm, hardness of the rubber = 40, and critical force $P_{cr} = 3220$ kN.

4.1 Rubber Backup Bearing

The parameters of backup supporters are: diameter = 400 mm, thickness of the laminated rubber $t_r = 5.0$ mm, number of layers of the bearing $n = 12$, thickness of the laminated steel plate $t_s = 1.5$ mm, hardness of the rubber = 40, and critical force $P_{cr} = 9360$ kN.

1. The value of Δ is fixed as 150 mm, the vertical load $P = 300$ kN, the value of Δ_0 is fixed as 0, 20, 35, 50 mm. Using Equations (21), (28) and (22), the ratio P_1/P can be calculated, where P_1 is the force in load-carrying bearing, and P is the total vertical force. In addition, the vertical deformation of the load-carrying bearing δ_v is calculated by using Equations (19) and (27). The computational results are listed in Table 20.

Table 20: P_1/P and Vertical Deformation δ_v

Pre-saving space of backup bearing	Δ_0 (mm)	0	20	35	50
Neglecting the decreasing of load-bearing area	P_1/P	0.810	0.804	0.803	0.801
	δ_v (mm)	0.137	0.133	0.130	0.128
Considering the decreasing of load-bearing area	P_1/P	0.627	0.621	0.617	0.614
	δ_v (mm)	0.297	0.277	0.266	0.256

As shown in Table 20, with the increase in the value of Δ_0 , the ratio P_1/P gradually reduces, but the extent of decrease is very small. For example, when the value of Δ_0 increases from 0 to 50 mm, neglecting the influence of reduction in effective load-carrying area, the ratio P_1/P reduces only by 0.51%. If the reduction in effective load-carrying area is considered, the ratio P_1/P reduces by 2.1%, which is larger than that on neglecting such kind of influence, namely 0.51%.

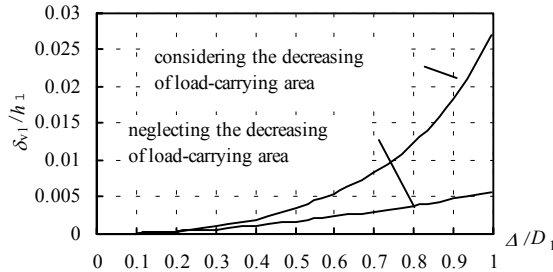


Fig. 10 Variation of δ_{v1} with horizontal displacement

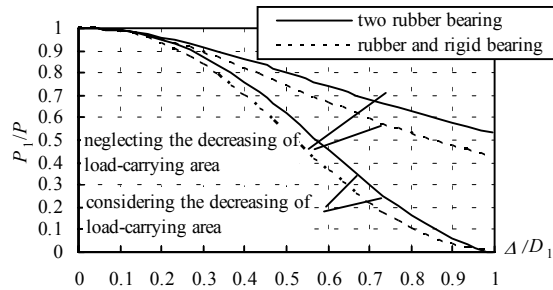


Fig. 11 Variation of P_1/P with horizontal displacement

From Table 20, it can be seen that the vertical deformation, δ_v , decreases with increasing Δ_0 . For example, as the value of Δ_0 increases from 0 to 50 mm, while neglecting the decrease in effective load-carrying area, the decrease of δ_v is 6.7%, whereas the decrease of δ_v is 14% on considering the decrease in effective load-carrying area.

2. The value of Δ_0 is fixed as 35 mm. For variable value of Δ , we calculate the ratio P_1/P and δ_v . The results are depicted in Figures 10 and 11. The vertical coordinate of diagram, shown in Figure 10, represents the proportion of vertical deformation of rubber bearing to its total height.

From Figure 10, we can see that increasing Δ causes the growth of δ_v . The upper curve in Figure 10 shows that if the decrease in the effective load-carrying area is taken into account, the increasing trend of δ_v , with increasing Δ , would be enhanced.

The vertical coordinate of diagrams, in Figure 11, shows the load carried by the load-carrying rubber bearing in the total vertical load. As illustrated in Figure 11, the force in load-carrying bearing reduces as Δ increases. However, the reduction apparently further accelerates when the influence of the decrease in effective load-carrying area is considered.

4.2 Rigid Backup Bearing

The dashed line, in Figure 11, presents the corresponding calculated results for rigid backup bearing, i.e. the axial force acting on load-carrying bearing, P_1 , reduces with increase in Δ . However, the value of P_1/P for the rigid backup bearing is relatively smaller than when both the load-carrying and backup bearing are rubber bearings, at the same value of Δ .

Figure 12 shows the change in axial force acting on rigid backup supporter with increasing horizontal displacement. It can be seen from Figure 12 that the vertical load of rigid backup bearing increases with

increasing Δ . Suppose that the frictional coefficient on the top of rigid backup bearing is μ . Then, the frictional force μP_2 of rigid backup bearing increases with increasing Δ as well.

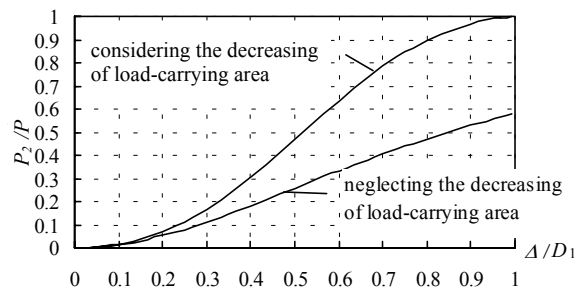


Fig. 12 Variation of P_2/P with horizontal displacement

THE COMPARISON OF PROTECTION OPTIONS

The rubber bearings in seismic base isolation layer make the natural period of the system consisting of the superstructure and the base isolation layer shift to longer side far beyond the dominant periods of normal ground motion accelerations and thus greatly reduce the seismic response of the superstructure. It is the rubber bearings which undergo considerable lateral deformations, and thus protect the superstructure by making it behave nearly like a rigid body. Since the rubber bearings in seismic isolation layer are key components for ensuring safety of the protected structure, the bigger ones are desirable. On the other hand, the rubber bearings, acting as vertical load supporters of the superstructure, need not be designed too large in order to make the base-isolated building have appropriately longer natural period. In particular, the option of large rubber bearings not only is expensive but is also unreasonable because that will shorten the natural period of the base-isolated building. If the size of the rubber bearings is not large enough to withstand the required lateral deformations induced by the maximum considered earthquake, to protect them from failure in such kind of an earthquake is important. The three types of safety protection measures for rubber bearing in base-isolated buildings proposed in this paper can be regarded as safety fortifications of second line of structural earthquake resistance which will play an important role for surviving the unexpected extreme earthquake at lesser cost.

1. Soft Pounding Protection

The effectiveness of soft pounding protection depends on what parameters have been selected in the protection system. In pre-setting space d , the lower limit should be guaranteed so that the isolator could not bump against the stopper during frequently-occurring earthquake, and the upper limit should be determined according to the deformation capacity of the rubber bearings. Generally, a relatively smaller value of d is preferable from the point of engineering practice.

The damping property of the buffer stopper can be represented by the ratio of its damping coefficient and that of the isolators. For different values of d and TN , the value of CR has different suitable ranges where the smaller value is preferable.

The value of TN , which represents the relative flexible property of the stopper, should not be too small. For normal structures, the effect of the soil-structure interaction can be neglected when we analyze base-isolated building with pounding protection. Therefore, in engineering design, we normally can use model II of the rigid foundation structure to replace model I in consideration of soil-structure interaction.

2. Stiffness-Variable Systems

Referring to the way discussed above, it is illustrated that the systems of stiffness variable protection may achieve very satisfactory controlling effect when the values of d and NK are adequate.

The stiffness property of the stiffness variable protection systems should be optimized deliberately from the mentioned three aspects, i.e., isolation layer, superstructure and construction cost. For different values of d , the value of NK has different suitable ranges where the small value is preferable.

Meanwhile, it is worth pointing out here that the systems of stiffness variable protection can be installed either on one side or on both sides of the base-isolated building.

3. Soft Landing Protection

The base isolation system, proposed here, consists of a load-carrying rubber bearing and an elastic or rigid backup supporter in parallel. It should be noted that the analysis aiming at soft landing protection system is primary and tentative because the rubber bearings and the backup supports distributed in isolation layer are respectively lumped as one component as shown in Figures 5 and 6. However, the vertical loading forces among various load-carrying rubber bearings are uneven and the global stability of the whole base isolation building is surely better than that of the individual ones, under action of dead load and lateral earthquake force simultaneously. Furthermore, the transmission of dead load from load-carrying rubber bearings to backup supports is inhomogeneous and the friction forces on the surfaces of backup supports, caused by the dead load transmitted from load carrying rubber bearings, are uneven as well. Hence, the real situation of the interaction behavior among load-carrying bearings and backup supports, is much more complex than that has been described above. But as a new approach and option of base isolation system the mentioned simple model should be a foundation for further study. As a supplemental measure, the combined system consisting of load-carrying rubber bearings and backup supporters with friction sliding surface has following advantages:

1. The backup bearing can protect the load-carrying bearing from losing its stability.
2. With a sliding plate, the backup bearing can supply variable frictional force to limit the displacement of the isolation layer.
3. Because the vertical force transfers gradually from load-carrying bearing to backup bearing, the bumping or impacting effect would be insignificant when large horizontal displacement happens.
4. For the load-carrying bearing, when its lateral deformation is small, because of large $P - \Delta$ effect, its horizontal stiffness is relatively small. In the case of large lateral deformations, its decreasing axial force causes reduction in $P - \Delta$ effect, thus its horizontal stiffness increases, and then the increase in displacement is restricted.

In summary, this system, making full use of the capacity of the rubber bearing and reducing the total cost of isolation system, usually is an economical and effective isolation system. To apply this system in engineering practice, more sophisticated dynamic analysis model and experimental work are needed. The creeping of load-carrying bearing under dead load and the optimization of parameters also need to be intensively studied. In addition, to bring this system into full play, the following aspects should be noticed:

1. The tolerable shear stain should be as large as possible, such as 500% or higher, and the adhesive strength of the steel plate and the rubber should be enough.
2. The backup bearing must be able to carry all of the vertical load and the horizontal shear force imparted by the sliding plate.
3. The frictional coefficient of the slide elements should be selected on the basis of analysis and comparison. The sliding displacement of the rigid backup bearing should match with the deformation capacity of the load-carrying bearing when its axial force is zero.
4. The value of P/P_{cr} (P is the total vertical load on superstructure that is entirely imparted on the load-carrying bearing before the lateral deformation takes place) should be appropriately selected. Avoid both swelling or inclining of the rubber bearing due to the excessively large P/P_{cr} and the transmission hampering of the force from load-carrying bearing to backup bearing due to an extremely small P/P_{cr} .
5. While designing the upper beams of isolation layer, one should pay sufficient attention to the fact that the vertical loads eventually will be carried by the backup bearings when large lateral displacement happens during the extreme earthquake. Also, necessary structural measures should be undertaken to ensure safety both for superstructure and bearing supports.

CONCLUSIONS

In the mentioned three types of rubber bearing protection measures, the common point of soft pounding and stiffness variable systems is using supplemental spring and damping devices to limit growth of the lateral displacement of rubber bearings in seismic isolation layer. Those will inevitably

induce some high frequency contents of vibration and then enhance structural shear forces and absolute acceleration responses. However, analyses have illustrated that the resulting unfavorable effect cannot counteract the displacement reduction of isolation layer brought by the seismic protection system. The difference between soft pounding and stiffness variable system is that the additional spring installed at ground stopper can be re-separated from base-isolated building in the soft pounding system, but in contrast, the additional spring is permanently fixed on building once it is connected with the building in stiffness variable protection system. In addition, the soft pounding system usually needs elastic stoppers and buffers but stiffness variable system only uses additional spring. Soft landing protection uses backup supporters to receive weight of superstructure when rubber bearing suffers excessive lateral deformation and loses its loading capacity or stability when subjected to an unexpected strong earthquake. During the course of load transmission and slippage along the top surface of the backup bearing, the base-isolated building would suffer bump and shock. However, such kind of complex phenomenon has not yet been included in the analysis model and thus more intensive research is needed on this aspect. Furthermore, in this paper, only a preliminary theoretical analysis has been carried out, and therefore, the shaking table experimental verification needs to be done in future. Compared with the soft pounding system through using stoppers and buffers as described above, the latter ones, i.e. stiffness variable system and the soft landing system are simpler, less expensive and easier to realize in practice. All these measures mainly suit to the case when the height of the isolation layer is short. Otherwise, the restrainer components including reaction walls, stoppers and backup supports should be very thick and large to make them have sufficient stiffness and strength.

ACKNOWLEDGEMENTS

This paper is funded by Natural Science Foundation of China under Grant No. 50178007 and also by Beijing Educational Committee. These financial supports are gratefully acknowledged. We also gratefully thank anonymous reviewers of this paper for their precious opinions and suggestions which were very helpful during the revision of this paper.

REFERENCES

1. Bruce, F.M. and Carlos, E.V. (1992). "Seismic Analysis of Base-Isolated San Bernardino County Building", *Earthquake Spectra*, Vol. 8, No. 4, pp. 605-633.
2. Buckle, I.G. and Kelly, J.M. (1986). "Properties of Slender Elastomeric Isolation Bearings during Shake Table Studies of a Large-Scale Model Bridge Deck" in "Proceedings of 2nd World Congress in Joints and Bearings Systems of Concrete Structures", Publication SP-94, American Concrete Institute, U.S.A., Vol. 1, pp. 247-269.
3. CABP (2001). "Seismic Design Code for Buildings", Report GB50011-2001 (in Chinese), China Architecture and Building Press, P.R.C.
4. CABR (1999). "Test Research Report of Mechanical Properties of Seismic Isolation Rubber Bearings for Buildings", Technical Report of Seismic Design Code (in Chinese), Institute of Earthquake Engineering, China Academy of Building Research, P.R.C.
5. Gent, A.N. (1964). "Elastic Stability of Rubber Compression Springs", *Journal of Mechanical Engineering*, Vol. 6, No. 4, pp. 318-326.
6. Griffith, M.C., Kelly, J.M. and Aiken, I.D. (1987). "A Displacement Control and Uplift Restraint Device for Base Isolated Structures", Report UCB/EERC-87/3, University of California at Berkeley, CA, U.S.A.
7. Han, M. (1997). "The Design Analysis Methodology and Engineering Application of Building Seismic Base Isolation System and Devices", Ph.D. Thesis (in Chinese), Institute of Geophysics, China Seismological Bureau, P.R.C.
8. Jean, Y., Lin, T.W. and Penzien, P. (1990). "System Parameter of Soil Foundation for Time Domain Dynamic Analysis", *Earthquake Engineering and Structural Dynamics*, Vol. 19, pp. 541-553.
9. Kelly, J.M., Beucke, K.E. and Skinner, M.S. (1980). "Experimental Tests of a Friction Damped Aseismic Base Isolation System with Fail-Safe Characteristics", Report UCB/EERC-80/18, University of California at Berkeley, CA, U.S.A.

10. Kelly, J.M. (1998). "The Analysis and Design of Elastomeric Bearings for Application in Bridges" in "Proceedings of the U.S.-Italy Workshop on Seismic Protective Systems for Bridges", Report MCEER-98-0015, SUNY at Buffalo, NY, U.S.A.
11. Koh, C.G. and Kelly, J.M. (1986). "Effects of Axial Loads on Elastomeric Bearings", Report UCB/EERC-86/12, Earthquake Engineering Research Center, University of California at Berkeley, CA, U.S.A.
12. Luan, M. and Lin, G. (1996). "2-DOF Lumped-Parameter Model of Dynamic Impedances of Foundation Soils", *Journal of Dalian University of Technology (in Chinese)*, Vol. 36, No. 4, pp. 477-482.
13. Nagarajaiah, S. and Ferrell, K. (1999). "Stability of Elastomeric Seismic Isolation Bearings", *Journal of Structural Engineering (ASCE)*, pp. 946-954.
14. Ohhira, M., Higaki, S., Teramura, A., Nakamura, T., Kobatake, M. and Hisano, M. (1990). "Earthquake Response Characteristics of Base-Isolated Building Models with Fail-Safe Devices", *Proceedings of 8th Japanese Earthquake Engineering Symposium*, Japanese Society of Soil Mechanics and Foundation Engineering, Tokyo, Japan, pp. 1719-1724.
15. Sun, L.M. and Goto, Y. (1996). "Simulations on Effectiveness of Energy Dissipating Buffer for Reducing Response of Bridge during Large Earthquake", *Proceedings of 11th World Conference on Earthquake Engineering*, Acapulco, Mexico, Vol. 7, pp. 23-28.
16. Wolf, J.P. and Somaini, D.R. (1986). "Approximate Dynamic Model of Embedded Foundation in Time Domain", *Earthquake Engineering and Structural Dynamics*, Vol. 14, pp. 683-703.
17. Zhou, X.Y., Han, M., Ma, D. and Zeng, D. (1997). "Stability Analysis and Strength Checking of Laminated Rubber Bearing", *Building Science (in Chinese)*, Vol. 13, No. 6, pp. 13-19.
18. Zhou, X., Han, M., Zeng, D. and Ma, D. (2000). "The Engineering Theory and Computation Method for Designing Isolation System of Rubber Bearing and its Composite Devices", *Proceedings of 12th World Conference on Earthquake Engineering*, Auckland, New Zealand.